

See discussions, stats, and author profiles for this publication at: <https://www.researchgate.net/publication/23456301>

Halogen bonding in 1,2-dibromo-4,5-dimethoxybenzene and 1,2-diiodo-4,5-dimethoxybenzene

Article in *Acta Crystallographica Section C Crystal Structure Communications* · December 2008

DOI: 10.1107/S010827010803309X · Source: PubMed

CITATIONS

4

READS

59

4 authors, including:

[Fabio Cukiernik](#)

University of Buenos Aires

51 PUBLICATIONS 750 CITATIONS

SEE PROFILE



[M. T. Garland](#)

University of Chile

402 PUBLICATIONS 3,498 CITATIONS

SEE PROFILE

Halogen bonding in 1,2-dibromo-4,5-dimethoxybenzene and 1,2-diiodo-4,5-dimethoxybenzene

Fabio D. Cukiernik,^{a,b} Andrés Zelcer,^{a,†} Maria Teresa Garland^c and Ricardo Baggio^{d,*}

^aDepartamento de Química Inorgánica, Analítica y Química Física, Facultad de Ciencias Exactas y Naturales, UBA, Buenos Aires, Argentina, ^bInstituto de Ciencias, Universidad Nacional de General Sarmiento, Buenos Aires, Argentina,

^cDepartamento de Física, Facultad de Ciencias Físicas y Matemáticas and CIMAT, Universidad de Chile, Santiago de Chile, Chile, and ^dDepartamento de Física, Centro Atómico Constituyentes, Comisión Nacional de Energía Atómica, Buenos Aires, Argentina

Correspondence e-mail: baggio@cnea.gov.ar

An interesting case of ‘halogen-bonding-promoted’ crystal structure architecture is presented. The two title compounds, $C_8H_8Br_2O_2$ and $C_8H_8I_2O_2$, have almost indistinguishable molecular structures but very different spatial organization, and this is mainly due to differences in the halogen-bonding interactions in which the different species present, *i.e.* Br and I, take part. The dibromo structure exhibits a π -bonded columnar array involving all four independent molecules in the asymmetric unit, with intercolumnar interactions governed by $C-Br\cdots Br-C$ links and with no $C-Br\cdots O/N$ interactions present. In the diiodo structure, instead, the $C-I\cdots O$ synthon prevails, defining linear chains, in turn interlinked by $C-I\cdots I-C$ interactions.

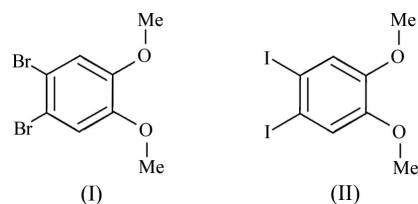
Comment

For many years, interest in the study of noncovalent interactions has been monopolized almost entirely by hydrogen bonding and, more recently, π - π and $C-H\cdots\pi$ interactions. The driving force for this interest was (and still is) the fundamental role these interactions play in molecular recognition, a chemical process basic to life itself but nowadays also closely related to many frontier technology enterprises. In the past few years, however, a different (though closely related) type of noncovalent interaction has begun to attract the scientist’s attention, the so-called ‘halogen bond’, where the main actor is a highly polarized halogen species. Under this wide umbrella, however, shelter a large variety of interactions of different aspects and behaviours; since only some of these

will be used in the present work, we will briefly introduce them here, directing the interested reader to more specific and qualified literature (*e.g.* Metrangolo *et al.*, 2007).

In particular, we shall deal with interactions of the $C-X\cdots O/N$ and $C-X\cdots X-C$ type (where X is a halogen). The main aspects of the former type are quite in tune with the conventional hydrogen bond, and accordingly its most conspicuous geometrical characteristics are (*a*) a rather large $C-X\cdots O/N$ angle ($> 150^\circ$) and (*b*) an $X\cdots O$ distance shorter than the sum of the van der Waals radii. The second type is rather more complex from a descriptive point of view, but the main aspects could be summarized as follows: if we denote the larger of the two $C-X\cdots X$ angles as θ_1 , and the smaller as θ_2 , then two types of $C-X\cdots X-C$ interactions can be envisaged (Desiraju & Parthasarathy, 1989), *viz.* the (so-called) *I1* interactions, which have $\theta_1 = \theta_2$, and the *I2* interactions, which have $\theta_1 \simeq 180^\circ$ and $\theta_2 \simeq 90^\circ$. In both cases, the $X\cdots X$ distance is shorter than the sum of the van der Waals radii.

The structures reported here, namely a couple of dihalogenated aryl derivatives, 1,2-dibromo-4,5-dimethoxybenzene (or dibromoveratrole), (I), and 1,2-diiodo-4,5-dimethoxybenzene (or diiodoveratrole), (II), correspond to some of the simplest systems where this type of interaction can take place. Diiodoveratrole is a versatile starting point in many chemical reactions, including the synthesis of electron-rich phthalocyanines, conductive polymers (Bhongale *et al.*, 2006) and catechol-based ligands (Kinder & Youngs, 1996). It belongs to the same family as diiodobenzene, but the methoxy substituents make this compound more electron-rich, thus rendering it more reactive towards electrophiles. The crystal structures of these closely related compounds are governed by a variety of nonbonding interactions, but the leading organizing forces are the above-mentioned ‘halogen bonds’.



The asymmetric unit of (I) is composed of four identical though nonequivalent molecules (*A-D*; Fig. 1), disposed one on top of the other in an almost perfect 4_1 arrangement, with a relative rotation of $\sim\pi/2$ and a graphitic translation shift (range ~ 3.64 – 3.80 Å; Table 1) when going from one to the next. This almost perfect columnar disposition is maintained by the fact that the array is continued *via* two inversion operations with their centres in the column axis, at $(0, 1, \frac{1}{2})$ and $(\frac{1}{2}, 0, 0)$ (marked as **x** and **y** in Fig. 2).

This preserves the alignment along the $[\bar{1}21]$ columnar direction of the π -bonded chain, while disrupting the pseudo- 4_1 stacking sequence, turning it into an $\dots ABCD-DCBA-ABCD\dots$ array (Fig. 2) with *D-D* and *A-A* related by inversion operations and at centre-to-centre distances [4.061 (1) and 4.227 (1) Å, respectively; Table 1] slightly

longer than typical. The columnar alignment seems to be the consequence of both π - π and dipolar C—O—C interactions; the dipole of the C3/O1/C7 ether group is almost aligned with that of the C4/O2/C8 group of the adjacent molecule, but with opposite sense (see Fig. 1).

Besides these π - π interactions connecting aromatic rings in a columnar-like array, the structure presents some other nonbonding interactions nearly at right angles to the column direction, of which the most important are the C—Br \cdots Br—C (type *I2*) halogen-bond contacts linking molecules with their nearest neighbours. The most relevant of these contacts ($d < 3.9$ Å) are shown in Fig. 1 and Table 2, all of them fulfilling the above-mentioned conditions for an *I2* interaction (first four entries) or for an *I1* interaction (last two entries). There are, in addition, a couple of nonconventional C—H \cdots O bonds,

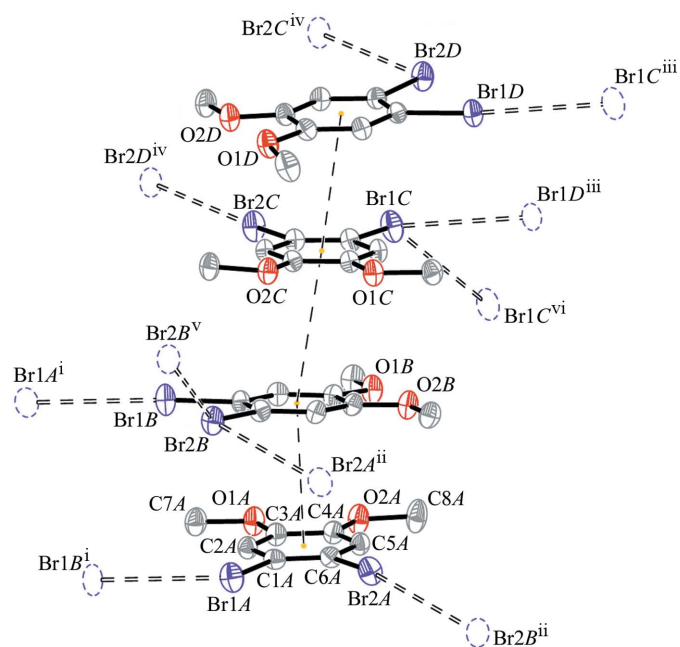
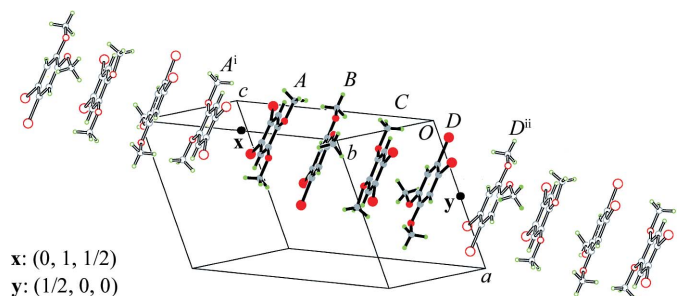


Figure 1

The asymmetric unit of (I), showing the four independent molecules (labelled A–D), with displacement ellipsoids drawn at the 40% probability level. Unlabelled atoms follow the same label sequence as molecule A. π - π bonds are represented by dashed lines connecting ring centres and Br \cdots Br interactions are represented by double-dashed lines. [Symmetry codes: (i) $-x + 1, -y + 2, -z + 1$; (ii) $-x, -y + 1, -z + 1$; (iii) $-x, -y, -z$; (iv) $-x + 1, -y + 1, -z$; (v) $-x + 1, -y + 1, -z + 1$; (vi) $-x, -y + 1, -z$.]



$x: (0, 1, 1/2)$
 $y: (1/2, 0, 0)$

Figure 2

A view of the packing of (I), showing the way in which a column is formed (see *Comment*).

presented in Table 3. All these interactions link neighbouring chains together into a densely connected three-dimensional structure (Fig. 3).

At a molecular level, (II) (Fig. 4) is almost identical to its Br analogue (I).

The main interactions in the structure are mediated by the halogen atoms, and in this respect the situation is highly asymmetric, atom I2 being much more active than I1. The strongest interaction is the head-to-tail link in which atom I2 makes a bifurcated contact with atoms O1 and O2 in a neighbouring molecule (Table 4 and Fig. 4), thus defining a

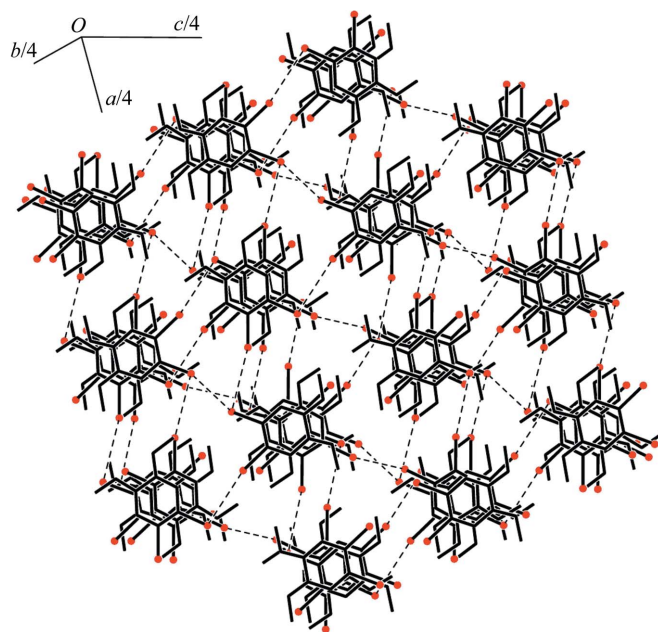


Figure 3

A view of the packing of (I), projected down $[\bar{1}21]$, the column direction, and showing the way in which parallel chains interact to form a three-dimensional structure.

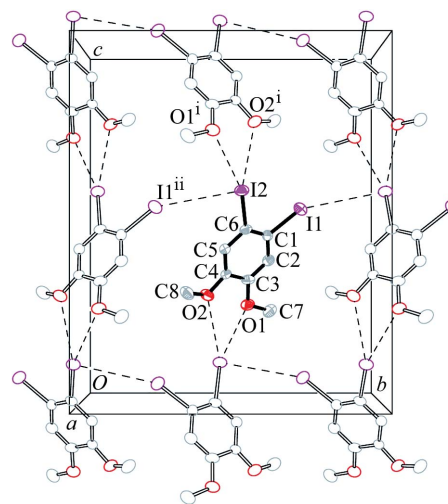


Figure 4

The two-dimensional structure in (II), parallel to (100), with displacement ellipsoids drawn at the 40% probability level. [Symmetry codes: (i) $-x + \frac{1}{2}, -y + 1, z + \frac{1}{2}$; (ii) $-x + \frac{1}{2}, y - \frac{1}{2}, z$.]

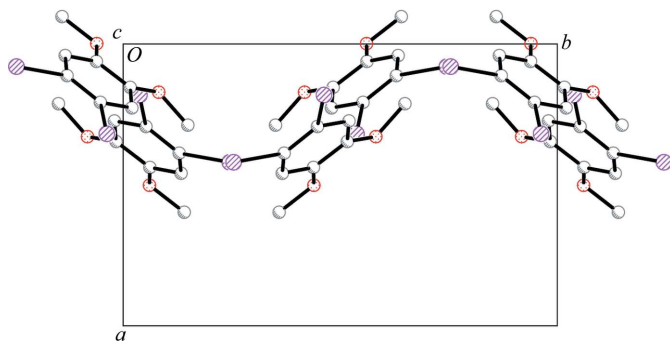


Figure 5
The same two-dimensional structure as in Fig. 4, viewed at right angles and revealing its 'wavy' character.

wavy chain running along the *b*-axis direction. These chains, in turn, are linked by a halogen–halogen contact (Table 5) into an also wavy two-dimensional structure parallel to (100). Both interactions are illustrated as broken lines in Fig. 4, where the two-dimensional array is shown; Fig. 5, in turn, exemplifies through a side view of the latter the wavy nature of the chain juxtaposition. Stacking of these two-dimensional elements promotes a couple of π interactions of different type, *viz.* a π – π contact (Table 6) and a C–H... π hydrogen bond (Table 7), which link the two-dimensional structures into a three-dimensional structure.

Thus, we have described two compounds that present almost indistinguishable molecular structures but which, in spite of the molecular similarities, give rise to completely different packing arrangements. This seems to be a result of the different strengths of the C–X...O and C–X...X–C interactions as a result of the change in the corresponding halogen species involved. In this respect, the C–Br...Br–C interaction appears to be much more feasible than C–Br...O [not a single example of the latter interaction is present in (I)]; conversely, the main synthon in (II), which leads to the formation of the chains, is constructed out of the C–I...O link, the C–I...I–C interaction appearing as second order and serving as an interchain linkage.

It is to be expected that these types of interactions will become more fully recognized and their incidence in crystal architectures will be analysed in more detail, so that better and more efficient *ab initio* molecular designs can be achieved through their statistical rationalization.

Experimental

Both title compounds were prepared by direct halogenation of dimethoxybenzene, using Br₂ and ICl for the dibromo and diiodo compounds, respectively.

For the synthesis of (I), in a three-necked 250 ml flask equipped with a thermometer and a pressure-compensated addition funnel were placed veratrole (10.141 g) and dichloromethane (125 ml) with a magnetic stirring bar. The flask was placed in an ice bath, and while the mixture cooled to 278 K, a hose with a funnel was attached to the remaining neck. The funnel was placed carefully facing down just over the surface of an Na₂CO₃ solution in such a way that the acid vapours generated would be neutralized by the carbonate. A solution

of Br₂ (8 ml) in CH₂Cl₂ (20 ml) was loaded into the addition funnel and added dropwise with continuous stirring over a period of 1 h. The ice bath was removed and the solution was stirred overnight. The contents of the flask were poured carefully into a separation funnel containing a solution of sodium bisulfite. The organic phase was washed with water, Na₂CO₃ and water again, dried over MgSO₄, and evaporated. The crude product was recrystallized from ethanol until no traces of the monobrominated product were detected by thin-layer chromatography, yielding 20.96 g (96%) of colourless crystals (m.p. 362–364 K).

The diiodo compound was prepared in a similar fashion to the brominated analogue. Namely, veratrole (9.106 g), dichloromethane (125 ml) and a magnetic stirring bar were placed in a 250 ml three-necked flask. The mixture was cooled to 278 K using an ice bath, and a pressure-compensated addition funnel and a system for the evacuation of the generated acidic vapours similar to that used in the synthesis of the dibromo compound were attached to the flask. A solution of ICl (22.5 g) in CH₂Cl₂ (20 ml) was loaded into the addition funnel and then added slowly dropwise (0.2 ml min⁻¹) with continuous stirring. The cold bath was removed and after 1 h of stirring at room temperature the solution was poured into a separation funnel containing sodium bisulfite. The organic phase was separated, washed with water, Na₂CO₃ and then water again, and dried over MgSO₄. The solvent was evaporated and the purple tar obtained was passed quickly through a fritted disc funnel filled with a short column of silica, eluting with a mixture of dichloromethane and cyclohexane. The almost colourless solution was evaporated and the resulting solid was recrystallized several times from ethanol, yielding 18.22 g (70.9%) of colourless blocks (m.p. 404–405 K).

Crystals of both compounds were obtained by slow evaporation of an ethanol solution of the corresponding dihalodimethoxybenzene. Depending on the speed of evaporation, crystals with dimensions ranging from less than a millimetre up to a centimetre were obtained. Both compounds showed ¹H NMR spectra consisting of two singlets, one corresponding to the aromatic H atoms (at 7.06 and 7.23 p.p.m. for the dibromo and diiodo compounds) and one corresponding to the methoxy H atoms at 3.83 p.p.m. Elemental analysis found (calculated) for C₈H₈Br₂O₂: C 32.6 (32.47), H 2.7% (2.72%); for C₈H₈I₂O₂: C 24.8 (24.64), H 2.1% (2.07%).

Compound (I)

Crystal data

C ₈ H ₈ Br ₂ O ₂	$\gamma = 101.0630$ (12) ^o
$M_r = 295.96$	$V = 1946.46$ (17) Å ³
Triclinic, $P\bar{1}$	$Z = 8$
$a = 10.1172$ (5) Å	Mo $K\alpha$ radiation
$b = 10.2052$ (5) Å	$\mu = 8.29$ mm ⁻¹
$c = 20.2764$ (10) Å	$T = 294$ (2) K
$\alpha = 104.1710$ (12) ^o	$0.16 \times 0.14 \times 0.14$ mm
$\beta = 98.9405$ (10) ^o	

Data collection

Bruker SMART APEX CCD area-detector diffractometer	30774 measured reflections
Absorption correction: multi-scan (SADABS; Bruker, 2002)	8656 independent reflections
$T_{\min} = 0.28$, $T_{\max} = 0.32$	5046 reflections with $I > 2\sigma(I)$
	$R_{\text{int}} = 0.033$

Refinement

$R[F^2 > 2\sigma(F^2)] = 0.036$	441 parameters
$wR(F^2) = 0.097$	H-atom parameters constrained
$S = 1.02$	$\Delta\rho_{\text{max}} = 0.44$ e Å ⁻³
8656 reflections	$\Delta\rho_{\text{min}} = -0.46$ e Å ⁻³

Table 1 π - π interactions (\AA , $^\circ$) for (I).

C_{g1} - C_{g4} are the centroids of the C1A-C6A, C1B-C6B, C1C-C6C and C1D-C6D rings, respectively, ccd is the distance between ring centroids, sa is the mean slippage angle (angle subtended by the intercentroid vector to the plane normal) and ipd is the mean interplanar distance (distance from one plane to the neighbouring centroid). For details, see Janiak (2000).

Group 1/group 2	ccd	sa	ipd
C_{g1}/C_{g1}^{vii}	4.061 (2)	25 (1)	3.66 (1)
C_{g1}/C_{g2}	3.639 (2)	4 (2)	3.62 (2)
C_{g2}/C_{g3}	3.802 (2)	21 (1)	3.55 (4)
C_{g3}/C_{g4}	3.670 (2)	13 (1)	3.58 (1)
C_{g4}/C_{g4}^{viii}	4.227 (2)	28 (1)	3.71 (1)

Symmetry codes: (vii) $-x, -y + 2, -z + 1$; (viii) $-x + 1, -y, -z$.**Table 2**C-Br...Br-C interactions (\AA , $^\circ$) for (I).

$\theta_1 = C'-X'\dots X''$ is the smallest of the two XB angles and $\theta_2 = X''\dots X''-C''$ is the largest of the two XB angles; the expected values are $\theta_1 \simeq 90^\circ$ and $\theta_2 \simeq 180^\circ$ (for I2 interactions) or $\theta_1 \simeq \theta_2$ (for I1 interactions). For details, see Desiraju & Parthasarathy (1989).

$C'-X'\dots X''-C''$	$C'-X'$	$C''-X''$	$X''\dots X''$	θ_1	θ_2
C1A-Br1A... (Br1B-C1B) ⁱ	1.887 (3)	1.886 (4)	3.7231 (7)	100.44 (13)	167.87 (11)
C6B-Br2B... (Br2A-C6A) ⁱⁱ	1.885 (4)	1.883 (4)	3.8901 (6)	97.45 (12)	160.75 (12)
C1C-Br1C... (Br1D-C1D) ⁱⁱⁱ	1.881 (4)	1.893 (4)	3.8051 (6)	98.06 (12)	165.23 (11)
C6D-Br2D... (Br2C-C6C) ^{iv}	1.889 (4)	1.899 (4)	3.7161 (6)	100.38 (12)	165.64 (11)
C6B-Br2B... (Br2B-C6B) ^v	1.885 (4)	1.885 (4)	3.4210 (9)	142.59 (11)	142.59 (11)
C1C-Br1C... (Br1C-C1C) ^{vi}	1.881 (4)	1.881 (4)	3.6291 (10)	135.24 (12)	135.24 (12)

Symmetry codes: (i) $-x + 1, -y + 2, -z + 1$; (ii) $-x, -y + 1, -z + 1$; (iii) $-x, -y, -z$; (iv) $-x + 1, -y + 1, -z$; (v) $-x + 1, -y + 1, -z + 1$; (vi) $-x, -y + 1, -z$.**Table 3**Hydrogen-bond geometry (\AA , $^\circ$) for (I).

$D-H\dots A$	$D-H$	$H\dots A$	$D\dots A$	$D-H\dots A$
C7A-H7AA...O2C ^{ix}	0.96	2.56	3.498 (5)	167
C8D-H8DA...O1B ^x	0.96	2.53	3.485 (5)	171

Symmetry codes: (ix) $x, y + 1, z$; (x) $x + 1, y, z$.**Compound (II)***Crystal data*

$C_8H_8I_2O_2$	$V = 2060.7 (17) \text{\AA}^3$
$M_r = 389.94$	$Z = 8$
Orthorhombic, <i>Pbca</i>	Mo $K\alpha$ radiation
$a = 8.993 (4) \text{\AA}$	$\mu = 6.07 \text{ mm}^{-1}$
$b = 13.882 (9) \text{\AA}$	$T = 294 (2) \text{ K}$
$c = 16.506 (4) \text{\AA}$	$0.32 \times 0.26 \times 0.16 \text{ mm}$

Data collection

Rigaku AFC-6 diffractometer	2023 independent reflections
diffractometer	1441 reflections with $I > 2\sigma(I)$
Absorption correction: ψ scan	$R_{\text{int}} = 0.039$
(North <i>et al.</i> , 1968)	3 standard reflections
$T_{\text{min}} = 0.18, T_{\text{max}} = 0.38$	every 150 reflections
2652 measured reflections	intensity decay: $< 2\%$

Refinement

$R[F^2 > 2\sigma(F^2)] = 0.042$	112 parameters
$wR(F^2) = 0.108$	H-atom parameters constrained
$S = 1.41$	$\Delta\rho_{\text{max}} = 0.82 \text{ e \AA}^{-3}$
2023 reflections	$\Delta\rho_{\text{min}} = -0.76 \text{ e \AA}^{-3}$

Table 4C-I...O interactions (\AA , $^\circ$) for (II).

For details, see Desiraju & Parthasarathy (1989).

$C-X\dots O$	$C-X$	$X\dots O$	$C-X\dots O$
C6-I2...O1 ⁱ	2.090 (7)	3.470 (5)	162.3 (2)
C6-I2...O2 ⁱ	2.090 (7)	3.321 (5)	148.3 (2)

Symmetry codes: (i) $-x + \frac{1}{2}, -y + 1, z + \frac{1}{2}$.**Table 5**C-I...I-C interactions (\AA , $^\circ$) for (II).

$\theta_1 = C1-X1\dots X2$ is the smallest of the two XB angles and $\theta_2 = X1\dots X2-C2$ is the largest of the two XB angles; the expected values are $\theta_1 \simeq 90^\circ$ and $\theta_2 \simeq 180^\circ$ or $\theta_1 \simeq \theta_2$. For details, see Desiraju & Parthasarathy (1989).

$C'-X'\dots X''-C''$	$C'-X'$	$C''-X''$	$X''\dots X''$	θ_1	θ_2
C6-I2...I1-C1 ⁱⁱ	2.090 (7)	2.089 (7)	4.231 (3)	91.7 (2)	146.1 (2)

Symmetry code: (ii) $-x + 1/2, y - 1/2, z$.**Table 6** π - π interactions (\AA , $^\circ$) for (II).

C_{g1} is the centroid of the C1-C6 ring, ccd is the distance between ring centroids, sa is the mean slippage angle (angle subtended by the intercentroid vector to the plane normal) and ipd is the mean interplanar distance (distance from one plane to the neighbouring centroid). For details, see Janiak (2000).

Group 1/group 2	ccd	sa	ipd
C_{g1}/C_{g1}^{iii}	4.036 (4)	22 (1)	3.75 (1)

Symmetry code: (iii) $-x, -y + 1, -z + 1$.**Table 7**C-H... π interactions (\AA , $^\circ$) for (II). C_{g1} is the centroid of the C1-C6 ring.

$D-H\dots A$	$D-H$	$H\dots A$	$D\dots A$	$D-H\dots A$
C7-H7A... C_{g1}^{iv}	0.96	2.90	3.747 (8)	147

Symmetry code: (iv) $x - \frac{1}{2}, y, -z + \frac{1}{2}$.

H atoms were placed at calculated positions [$C-H = 0.93$ (aromatic) and 0.96\AA (methyl)] and allowed to ride; methyl groups were also allowed to rotate. $U_{\text{iso}}(\text{H})$ values were set at $xU_{\text{eq}}(\text{host})$ [$x = 1.2$ (aromatic) and 1.5 (methyl)].

For (I), data collection: SMART (Bruker, 2001); cell refinement: SAINT (Bruker, 2002); data reduction: SAINT. For (II), data collection: MSC/AFC Diffractometer Control Software (Molecular Structure Corporation, 1988); cell refinement: MSC/AFC Diffractometer Control Software; data reduction: MSC/AFC Diffractometer Control Software. For both compounds, program(s) used to solve structure: SHELXS97 (Sheldrick, 2008); program(s) used to refine structure: SHELXL97 (Sheldrick, 2008); molecular graphics:

SHELXTL (Sheldrick, 2008); software used to prepare material for publication: *SHELXTL* and *PLATON* (Spek, 2003).

We acknowledge the Spanish Research Council (CSIC) for providing us with a free-of-charge license to the CSD system (Allen, 2002) and the donation of a Rigaku AFC-6S four-circle diffractometer by Professor Judith Howard. We also thank Raul Garay (UNSur) for interesting comments about halogen bonding, ANPCyT (PICT25409) and UBACyT (EX219) for financial support, and CONICET for a PhD fellowship to AZ. FDC is a member of the research staff of CONICET.

Supplementary data for this paper are available from the IUCr electronic archives (Reference: UK3001). Services for accessing these data are described at the back of the journal.

References

- Allen, F. H. (2002). *Acta Cryst.* **B58**, 380–388.
- Bhongale, C. J., Yang, C. H. & Hsu, C. S. (2006). *Chem. Commun.* pp. 2274–2276.
- Bruker (2001). *SMART*. Version 5.624. Bruker AXS Inc., Madison, Wisconsin, USA.
- Bruker (2002). *SAINT* (including *SADABS*). Version 6.22a. Bruker AXS Inc., Madison, Wisconsin, USA.
- Desiraju, G. R. & Parthasarathy, R. (1989). *J. Am. Chem. Soc.* **111**, 8725–8726.
- Janiak, C. (2000). *J. Chem. Soc. Dalton Trans.* pp. 3885–3898.
- Kinder, J. D. & Youngs, W. J. (1996). *Organometallics*, **15**, 460–463.
- Metrangolo, P., Resnati, G., Pilati, T., Liantonio, R. & Meyer, F. (2007). *J. Polym. Sci. A*, **45**, 1–15.
- Molecular Structure Corporation (1988). *MSC/AFC Diffractometer Control Software*. MSC, The Woodlands, Texas, USA.
- North, A. C. T., Phillips, D. C. & Mathews, F. S. (1968). *Acta Cryst.* **A24**, 351–359.
- Sheldrick, G. M. (2008). *Acta Cryst.* **A64**, 112–122.
- Spek, A. L. (2003). *J. Appl. Cryst.* **36**, 7–13.